

# On the growth of two dimensional crystals:

## 2. Assessment of kinetic theories of crystallization of polymers

David M. Sadler

*H. H. Wills Physics Laboratory, University of Bristol, Tyndall Avenue, Bristol BS8 1TL, UK*

*(Received 9 April 1986; revised 7 November 1986; accepted 13 February 1987)*

Results of analyses of growth processes on two dimensional (2d) crystals are applied to kinetic theories for crystallization of polymers. The purpose is firstly to assess the rate equation methods of calculation which have been used for nucleation (LH) theories, and secondly to estimate free energies of steps  $\sigma_n$  on the growth faces of the crystal lamellae in a manner independent of detailed models. A systematic critique is then given of the LH theories, on the basis both of the simulation results and previous work. The range of validity of the calculations used in nucleation theories, using rate equation approaches, is assessed in the light of the effects of fluctuations in step positions and of simulation results (Part 1, ref. 1). The simulation results are given in terms of  $\sigma_n$  and the free energy  $\delta f$  for adding stems at niche sites. It is pointed out that, for those nucleation theories which predict  $l$  values in line with experiment,  $\delta f/kT \lesssim 1$ . For this range of  $\delta f$  values the density of steps on the surface which is found from simulation results is fairly near the equilibrium values. The predicted step densities in Regime II of (the nucleation theory) is only  $2^{-1/2}$  times the equilibrium density (for low step densities). This difference is discussed in terms of a near approach to equilibrium which is mediated by the growth process. Part 1 emphasized the close connection between growth rates and step densities. The dependence of both on  $\sigma_n$  is very similar for the simulation results and for the Regime II result (for average spacings between steps greater than about four lattice spacings). For rougher surfaces than this, the growth rate saturates and reaches a plateau at  $\sigma_n = 0$ . This is readily interpreted since the step density also saturates. This result is contrasted with that of Regime III (for rough surfaces) which predicts an even stronger dependence of growth on  $\sigma_n$  than in Regime II. The discrepancy between the simulation results and Regime III is discussed in detail, and it is pointed out that the prediction of growth in the absence of a thermodynamic driving force is associated with violation of the principle of microscopic reversibility. The applicability of kinetic models is also discussed. Morphological observations, as discussed in more detail elsewhere, seem incompatible with LH theories. The growth rate plots (rate on a log scale against  $(T\Delta T)^{-1}$  or against  $\sigma_n$ ) are not fully explained by them: only completely straight growth plots can be explained, or smoothly curved convex ones (in terms of a Regime I/II transition, but even for this explanation to be valid the relevant morphological evidence must be disregarded). Concave or sharply kinked growth plots cannot be directly explained in this way. Alternative kinetic models, based on rough growth surfaces and pinning (as a consequence of molecular connectivity) are also discussed briefly in view of the range of experimental evidence. A review is included of other comparisons of experiment with LH theory, including the lack of crystal size effect on the growth rate and the analysis of growth rates of poly(ethylene oxide). It is concluded that the basic hypothesis of LH theories, that  $\sigma_n$  is generally large compared with  $kT$  and that  $\sigma_n$  increases linearly in a steep manner with the lamellar thickness, are not consistent with the experimental evidence.

(Keywords: crystallization; kinetic theories; nucleation; pinning; two-dimensional crystals; regime theory; chain folding; morphology; simulation)

### INTRODUCTION

There are at present several reasons to reassess the kinetic theories for predicting lamellar thicknesses and growth rates of polymer crystals. This paper applies results of a simulation analysis<sup>1</sup> in order: (1) to assess the validity of the rate equation analyses which have been used in 'nucleation' (or LH) theories<sup>2-21</sup>; (2) to examine the fundamental premises of such theories. The premises are that the free energy  $\sigma_n$  for steps on the lamellar growth faces rise to values *large compared with  $kT$*  and that  $\sigma_n$  *increases linearly with the lamellar thickness  $l$* . There is also the related question of whether stems (chain sequences traversing lamellae) can be treated as single units, or whether a shorter fundamental unit should be considered. In this paper attention will be concentrated on the two

clearly distinguished cases of models based on complete stems (and with  $\sigma_n/kT \gg 1$ ) and those based on  $\sigma_n/kT \approx 1$ <sup>22-30</sup>. It has been argued previously<sup>22</sup> that in order for  $\sigma_n/kT \approx 1$  the growth faces must be rough, and that short chain segments must be considered. (The model of Point<sup>13</sup> can be considered as intermediate between the two cases discussed here.)

A reassessment of theories of polymer crystallization is suggested by a number of discrepancies between LH theories and observations. On one hand, the basic premise (of large  $\sigma_n/kT$ ) is in very clear conflict with the observed shapes of crystals: there is no sign that re-entrant corners enhance the growth to anything like the extent predicted<sup>22,23,25,27</sup>. This line of argument is based

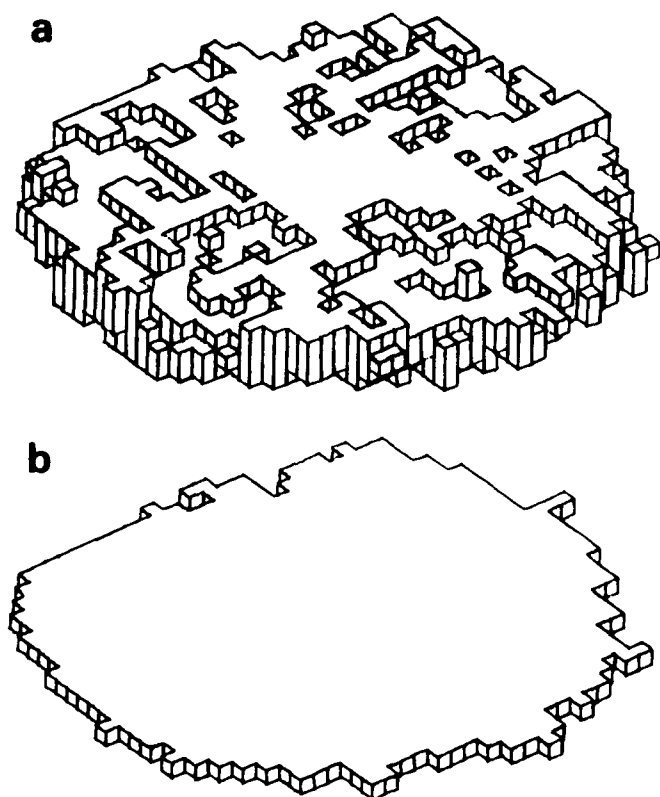


**Figure 1** (a) A simulated crystal using a short length of chain as the basic unit<sup>22,24,25,28-30</sup> (chain direction vertical). The bond energy both vertically and horizontally is given by  $\epsilon/kT=1.4$ . No solid on solid restriction is imposed other than in the vertical direction, and further results using this procedure will be published elsewhere. (b) 2d crystal: which can be used for some purposes to model the more complicated situation

on advances in the understanding of crystal growth surfaces for non-polymers<sup>31-34</sup>. Other discrepancies have been known for some years: for example Point, Colet and Dosiere<sup>35</sup> have re-examined carefully the relationship between growth rate  $G$  and lateral crystal size. They fail to observe any dependence of  $G$  upon size as might have been expected. A second example is the failure to observe<sup>36,37</sup> large  $l$  values at large supercoolings ( $\Delta T$ ) which is predicted by many LH theories (e.g., the ones including the physically significant effect of fluctuations in stem lengths<sup>3-6</sup>). A third example is the difficulty<sup>38</sup> in accounting for relative growth rates of oligomeric poly(ethylene oxide) of different crystal thicknesses<sup>39</sup>.

LH theories have used rate equation analyses (REA) which require the processes involved in crystallization to be sequential. The first application of simulation results<sup>1</sup> is to investigate how good an approximation this is, given the basic premises of LH theories. The concern is Regimes II<sup>10</sup> and III<sup>15</sup>, which correspond to more than one step (on average) on each crystal growth face. For Regime II the simulation results agree approximately with those of REA, though there is a discrepancy of  $2^{1/2}$  in the magnitude of the growth rate  $G$ . It is also suggested that a result similar to Regime II is more general than implied by the assumption of the REA and that it can be derived analytically much more simply than hitherto. There is no such agreement for Regime III, and since Regime III has become of considerable importance in analysing growth rate data, the disagreement is discussed in detail.

The second application of the simulation results<sup>1</sup> is

entirely distinct from the first and addresses the central issue of the magnitudes of  $\sigma_n$ . It is intended to apply to *any* model where the free energy of a step on the growth face can be assigned a particular numerical value. This point is illustrated in Figures 1 and 2, which show (Figures 1a and 2a) two crystals simulated with short chain sequences as introduced elsewhere<sup>22-27</sup>. Figures 1b and 2b show 2d models (projections of those in Figures 1a and 2a) which for *some* purposes can be treated as approximately equivalent. In order to make the link between models in (a) and (b) in Figures 1 and 2 it is sufficient to assign a *free* energy  $\sigma_n$  to a step which crosses from the top to the bottom of the crystal so as to introduce a niche in the outline shape. For the models in (a), of course, an entropy will be involved in  $\sigma_n$  since the steps can have jogs as they cross the growth face.

For the sake of completeness, this paper also reviews some of the comparisons between predictions of LH theories and experiments which do not involve morphology and briefly describes the current status of the recently developed models<sup>22,24,25,28,29</sup> which involve growth faces which can be rough and 'pinning' (the consequence of molecular connectivity).

#### (1) NUCLEATION AND NUCLEATION THEORIES

It is necessary for clarity to consider the question of nomenclature and how the term 'nucleation' should be used in connection with the kinetic theories used to

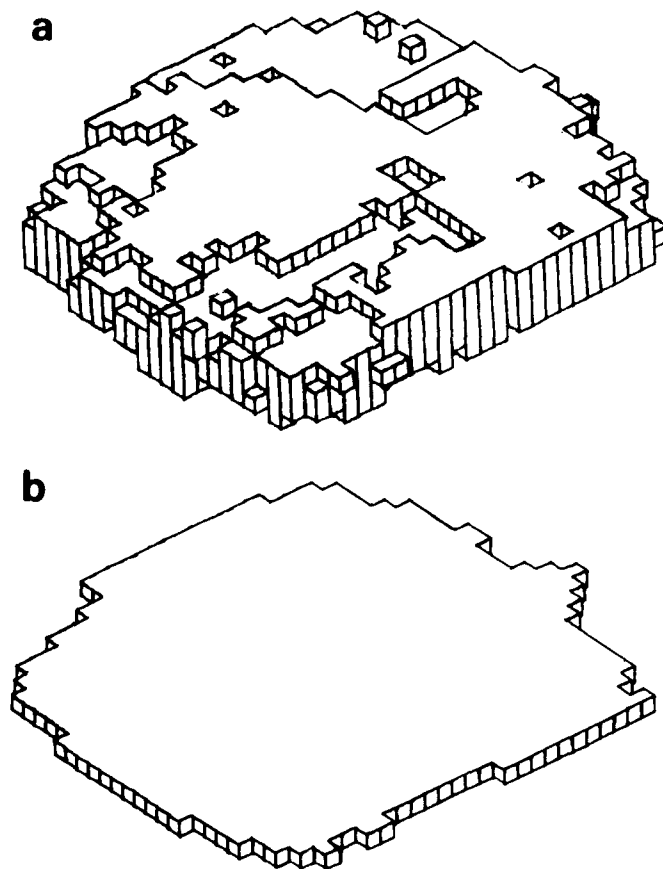


**Figure 2** Equivalent results as in Figure 1, but with  $\epsilon_n/kT=2.0$ . Note the decreased roughness and growth face curvature compared with Figure 1

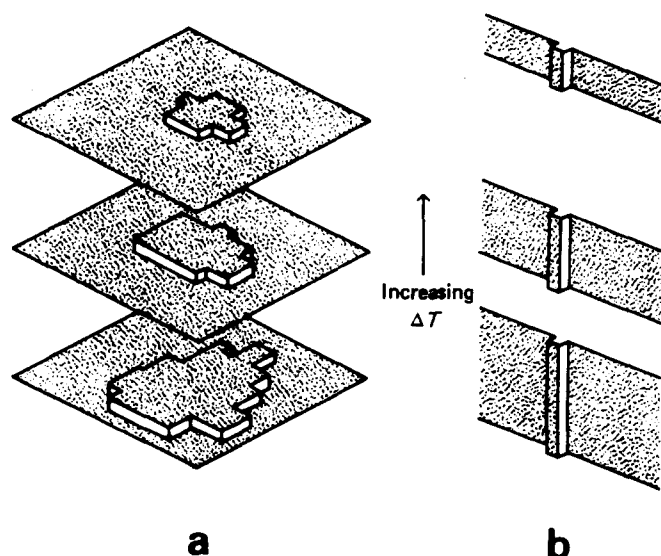


**Figure 3** Diagrams relevant to the definition of nucleation. (a) shows schematically the critical nucleus on 2d surfaces for three different  $\Delta T$ . (b) shows additions of single stems to smooth surfaces, as in LH models, for three different  $\Delta T$

explain chain folding (see also ref. 26). Nomenclature is to some extent a question of choice, but whichever usage is adopted it is important that it should be unambiguous. For polymer crystallization there is a problem in nomenclature since there is an almost continuous spectrum of behaviour that can be expected for growth on to a surface of small finite width (on the lamellar perimeter). If the word 'nucleation' is to be used it can only refer to one limiting case of this spectrum, distinguished from other cases by little more than the quantitative values of some of the parameters involved.

A nucleation process<sup>40,26</sup> on a surface (for non-polymers) has always been considered to correspond to the creation of patches, with steps around their perimeters, on a surface which would have no steps crossing it in the absence of a thermodynamic driving force (i.e., no steps in the case of equilibrium between crystal and non-crystal). Before the patch can grow with a small chance of removal, it must pass a 'critical' size, for which the free energy  $\Delta F^*$  is at a maximum. Crucial to nucleation is that  $\Delta F^*$  should approach infinity as the driving force goes to zero (hence the zero step density at equilibrium). Figure 3a shows schematically critical patch sizes for three different values of supercooling  $\Delta T$ . For a given 1d surface on a 2d crystal  $\Delta F^*$  is constant and hence nucleation in this sense does not occur<sup>26</sup>. However, LH theories consider lamellar surfaces whose thicknesses are larger as the supercooling  $\Delta T$  is smaller, and the width of the patches which form on them also increases (Figure 3b). In this rather limited sense, because of the similarity between Figures 3a and b, LH theories can be said to be based on a kind of nucleation process. When  $\sigma_n$  is as large as it generally is in nucleation theories ( $\geq 10kT$ ) the process of growth has a certain similarity to nucleation (1d nucleation) since patches form and grow systematically outwards just as do nuclei on 2d surfaces (see Part 1<sup>1</sup> and sections (2) and (4) in this paper). In these two ways there are certainly connections between LH theories and nucleation. However, it is probably misleading to use 'nucleation' as a synonym for 'attachment on a surface so as to increase the surface area'

(e.g., on a flat surface), because one is then led to the conclusion that all conceivable models would involve nucleation.

In this paper the term nucleation, or LH, theory is used simply to indicate a particular magnitude and  $l$  dependence of  $\sigma_n \cdot 2\sigma_n$  is considered the principal contribution to  $\Delta F^*$ . The free energy  $\Delta F^*$  for adding such a new patch must increase with  $l$ : specifically  $\sigma_n$  increases linearly with  $l$ , with a constant of proportionality sufficiently large that (for example)  $\sigma_n$  for PE rises to  $30kT$  or more (for  $l = 300 \text{ \AA}$ ).

Nucleation theories do not presume any particular theoretical concepts or qualitatively distinctive physical processes which do not occur in other approaches (e.g., the ones with rougher growth surfaces). On the other hand, models for molecular arrangements which can be used to justify nucleation (large  $\sigma_n$ ) theories are quite different from those used for rougher growth surfaces (smaller  $\sigma_n$ ).

LH theories are also kinetic theories, since they explain chain folding as a state of fast growth rather than of global free energy minimum. However they are not the only kinetic theory possible—roughness/pinning models are also kinetic as opposed to equilibrium.

## (2) THE 2d MODEL AND BASIC EQUATIONS

These are described more fully in Part 1<sup>1</sup>. The model uses a 2d square lattice of repeat distance  $a$ , with additions and removals according to the solid-on-solid (SOS) restriction. Surface sites are labelled 0–2 according to the number of lateral neighbours: type 0 correspond to 'adsorbed' units, type 2 to sites such as on smooth surfaces, and 1 to niches which are not adjacent to adsorbed units. Niches are steps on a 1d surface. Energy is calculated from nearest neighbour bonding only. The ratios of on and off rate constants  $A_i$  and  $B_i$  are given by:

$$B_0/A_0 = e^{(2\sigma_n - \delta f)/kT} \quad (1)$$

$$B'_1/A_1 = e^{-\delta f/kT} \quad (2)$$

$$B_2/A_2 = e^{-(2\sigma_n + \delta f)/kT} \quad (3)$$

for LH theories:

$$B_2 = 0$$

$$A_2 = A_1 \quad (3a)$$

$\delta f$  is the free energy fall when a unit is added to a niche site.

The way the energy depends on the configuration will determine how  $\sigma_n$  and  $\delta f$  depend on temperature. An additional degree of choice is available which depends on the details of the free energy barriers for the conversion of one configuration to another ('apportioning', see Part 1). The simulation work<sup>1</sup> put all the  $A_i$  equal, whereas the LH theories generally put  $B_0 = B'_1$ . This difference should not be important for many of the results in the limit of particular interest here, viz. approximate correspondence to equilibrium. All the analyses discussed here are equivalent to  $\psi = 0$ <sup>12</sup> (barrier height for addition independent of supercooling).

A strictly 2d model can be treated with reference to bonds of energy  $\varepsilon$  in two directions only:

$$\delta f = 2\varepsilon \delta T/T_m \quad (4)$$

$T_m$  is the melting point of the 2d crystal and  $\delta T$  is  $T_m - T$ .

This paper will also involve the application of 2d models to chain folding for which the formulation of the model is formally 3d, in which case:

$$\delta f = a^2 l h \Delta T / T_m^\circ - q \quad (4a)$$

$$= a^2 h \Delta T (l - l_m) / T_m^\circ \quad (4b)$$

where  $h$  is the heat of fusion per volume and  $q$  the free energy associated with the stem ends.  $T_m^\circ$  is the melting point of the 3d crystal with  $l$  infinite and  $\Delta T = T_m^\circ - T$ .  $l_m$  is the thickness of the crystal which would melt at  $T$ . A characteristic of LH theories is a strong dependence of  $\sigma_n$  on  $l$ , e.g.:

$$\sigma_n = a l \sigma \quad (5)$$

where  $\sigma$  is the (lateral) surface free energy per area. From equation (5) accepted values for  $\sigma^{12}$  would give very large  $\sigma_n/kT_m^\circ$  values; e.g., 10 ( $l = 100 \text{ \AA}$  for polyethylene (PE)) or 30 ( $l = 300 \text{ \AA}$ ). The effective  $\sigma_n$  values which are used are often less than this however, since the first stem to add to a smooth surface ('type 0') usually is not allocated a free energy associated with the end of the stem (subsequent stems are)\*. Hence:

$$\sigma_n(\text{effective}) = a l \sigma - q \quad (6)$$

This is the free energy difference between adding at smooth compared with niche sites. This brings the  $\sigma_n/kT_m^\circ$  value for  $l = 100 \text{ \AA}$  down to 4.3. (The average distance  $\lambda$  between niches, for equilibrium, is then about  $100a$ .) Equation (6) can give negative  $\sigma_n$  (e.g., for  $l = 50 \text{ \AA}$  in PE).

The addition and removal of stems from niche sites will involve separate events whose occurrence will be largely at random. An analysis<sup>1,7</sup> of the lateral niche movement as a biased one dimensional random walk leads to definition of a quantity  $d$  which characterizes the fluctuations in niche positions. It is that niche displacement necessary for the centroid of the probability distribution for the niche to be equal to its width. The width is defined as the distance from the centroid necessary for the distribution to fall to  $e^{-1}$  of its maximum value.

$$d = 4a / \sinh(2\delta f / kT) \quad (7)$$

for  $\delta f / kT_m \lesssim 1$ :

$$d = 2akT / \delta f \quad (7a)$$

For  $d \ll \lambda$  the growth has similarities to nucleation on 2d surfaces. For this regime of '1d nucleation' fluctuations do not significantly affect the interaction and annihilation of niches. For example new patches of one additional layer will fluctuate in size before they become effectively permanent (some will fluctuate back and be removed entirely). A probability  $i$  per unit width of crystal surface (measured in numbers of lattice sites) for the creation of a new patch can be defined, as long as the probability of a patch being entirely removed is small by the time it is likely to encounter another one.  $d$  characterizes the fluctuations and  $\lambda$  the probability of encountering another niche.  $i$  is then given by the result of a rate

equation analysis, for the sequence of states the first of which corresponds to one type 0 stem and subsequent states to 2, 3, etc., stems adjacent to each other:

$$i = A_0(1 - B'_1/A_1)/(1 - B'_1/A_1 + B_0/A_1) \quad (8)$$

for the case  $B'_1 = B_0$ :

$$i = A_0(1 - B'_1/A_1) \quad (8a)$$

The average niche spreading rate  $g$  (in stems per unit time) is given by:

$$g = A_1 - B'_1 \quad (9)$$

for one of the cases of interest here, Regime II,  $\lambda \ll L$  where  $L$  is the lateral width of the crystal, the growth rate in layers per unit time  $G(\text{II})$  is given by<sup>10,11</sup>

$$G(\text{II}) = (2ig)^{1/2} \quad (10)$$

If equation (8a) is used for  $i$ :

$$G(\text{II}) = (A_1 - B'_1)(2A_0/A_1)^{1/2} \quad (11)$$

Equations (10) and (11) are based on the growth rate being the product of the niche density and the average rate of niche spreading, measured in lattice sites per unit time:

$$G = C_1 g \quad (12)$$

$C_1$  is the fraction of surface sites which are of type 1. Equation (12) applies for the case  $\lambda \gg a$ .

For Regime II it has been proposed hitherto that the steady state value of  $C_1$  is determined on the basis of a balance between niche creation at patches and niche encounters (mutual annihilation). It was pointed out in Part 1 that this value of  $C_1$  is just  $2^{-1/2}$  times the equilibrium value of  $C_1$ . A 'near equilibrium' result based on equation (12) gives:

$$G(\text{near equilibrium}) = 2(A_1 - B'_1)(A_0/A_1)^{1/2} \quad (13)$$

$$= 2(ig)^{1/2} \quad (13a)$$

This simple derivation of a result similar to Regime II differs from the original derivation in that it is not based on the microscopic processes giving rise to the equilibrium (niche creation at patches, and annihilation when niches encounter each other). It seems clear that the factor of  $2^{1/2}$  distinguishing equations (11) and (13) arises from the neglect of cavity creation in the Regime II analysis.

*Note on the units of  $i$   $g$   $G$  and  $\beta$*

In contrast to most of the original LH publications,  $i$   $g$   $G$  and  $\beta$  in this paper are normalized to the dimensions of the lattice, for example  $G$  is the growth rate of number of new layers per unit time.  $\beta$  is the rate of incidence of new units per existing lattice site. Hence the dimensions of the lattice (widths of stems) do not feature directly in the equations. The ratio  $i/g$ , relevant to morphology (section (11) subsection (ii)), is then the ratio of net rates of addition to flat and corner sites (types 0 and 1 respectively). 1d nucleation ( $\sigma_n/kT \gg 1$ ) corresponds to  $i/g \ll 1$  (e.g.,  $\sigma_n/kT = 30$  gives  $i/g \approx 10^{-26}$ ).

### (3) $\delta f$ IN LH THEORIES: THE MECHANISM CONTROLLING $l$

In LH theories the  $\delta f$  values are not determined directly by the conditions of crystallization, but depend on the  $l$

\* If a stem end free energy is not allocated for type 0 creation of sites, this will affect the free energy of the final crystal. This effect will be most significant when a substantial fraction of the stems in a crystal were added by additions which create type 0 sites, i.e., for Regime III (see below). In this case  $\delta f$  should be modified accordingly before comparisons are made with simulation results, though in practice this is not an effect which is of concern here.

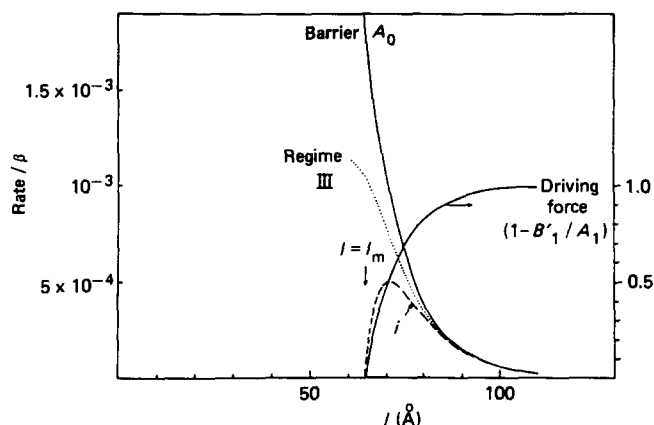


**Figure 4** Plots relevant to LH theories, as a function of stem length. Solid lines refer to  $A_0$  and  $(1 - B_1'/A_1)$  whose product gives one of the formulae for the nucleation probability  $i$  per surface site (shown by the dashed line (cf. Figure 1 of Frank and Tosi<sup>3</sup>)). The case of  $B_1' = B_0$  is chosen. The dotted line refers to the total flux for the Regime III analysis<sup>15</sup>. The values of thermodynamic quantities are appropriate to polyethylene<sup>12</sup>,  $\Delta T/T_m^\circ = 0.1$

value which itself is determined by the conditions. The process by which  $\delta f$  is determined is given in a form suggested by Frank and Tosi<sup>3</sup>, from which it is clear that the results should be general for a wide range of nucleation theories. The growth rate is closely related to the nucleation rate  $i$ , which can be considered the product of a 'barrier' term  $A_0$  and a 'driving force' term  $(1 - B_1'/A_1)$  (see equation (8a)). In order to specify all  $A$  and  $B$  values the apportioning must be defined (see refs. 1 and 3). The case considered here in detail is  $\psi = 0$ , i.e., the  $A$ 's independent of supercooling. In this section the dependence on  $\sigma_n$  is put into  $A_0$ :

$$A_0 = \beta e^{-2\sigma_n/kT} \quad (14)$$

This can be interpreted as the Boltzmann probability for generating a pair of niches (Figure 3b). The value of  $l$  obtained from these theories is weighted heavily by that  $l$  value which maximizes the product.

The result is clear from a consideration of Figure 4; the maximum value for  $i$  is likely to be at  $l$  values much smaller than corresponding to the saturation of the driving force term. The same conclusion is reached if the maximization is performed algebraically as follows.

For the present purposes the nucleation rate  $i$  (equation (8a) and ref. 2 for LH theories will be considered:

$$i = A_0(1 - e^{-\delta f/kT}) \quad (15)$$

$\delta f$  is given by equation (4).  $A_0$  is given by equation (14). The  $l$  value is usually calculated as an average which is weighted according to its corresponding growth rates; for  $l$  to be near  $l_m$  the result is:

$$l \simeq l_m + kT/a\sigma \quad (16)$$

Alternatively, the  $l$  value corresponding to maximum growth rate could be considered:

$$l \simeq l_m + kT/2a\sigma \quad (16a)$$

For the LH theories the quantity  $a\sigma$  is large compared with  $kT$  (it is related to  $\sigma_n$ ), so that  $kT/a\sigma$  is small compared with  $l$ . The value of  $\delta f$  corresponding to the average  $l$  value can now be calculated from equation (4b):

$$\delta f/kT = \frac{\Delta T}{T_m^\circ} \frac{(ha^2l)}{(\sigma al)} \quad (17)$$

$(ha^2l)$  is the heat of fusion per stem, and  $(\sigma al)$  is the stem surface free energy (e.g., corresponding to one side of a prism representing a stem). These two quantities are clearly related; in the simple case of a 2d model with rigid units the former would be four times the latter. (For accepted values of  $\sigma$  and  $h$ <sup>12</sup> the ratio for PE is 8.9.)  $\Delta T/T_m^\circ$  is usually 0.1 or smaller, so that equation (17) would give  $\delta f/kT$  of no more than unity (and often less: typical values are 0.89 for PE with  $\Delta T/T_m^\circ = 0.1$  and 0.44 for PE with  $\Delta T/T_m^\circ = 0.05$ ).

This section describes the simplest form of LH theory, applicable to an ensemble of crystals of constant  $l$ . Further developments allow for fluctuations of  $l$  within the same crystal<sup>3-6</sup>. The growth rate is calculated from the nucleation rate  $i$  and average step spreading rate  $g$  from formulae such as in equation (10). It is customary however to consider only  $i$  for a calculation of the preferred  $l$  value.

#### (4) THE 1d NUCLEATION CRITERION FOR LH THEORIES

The lowest  $\sigma_n/kT_m$  values in LH theories for PE are about 2.4 ( $\lambda \simeq 10a$ ), but generally they are much higher (up to 20–30), and  $\lambda$  is very much higher even than  $10a$ . On the other hand  $\delta f/kT_m$  is of the order of unity (see the previous section). From equations (7) one can see that the fluctuation distance  $d$  is unlikely to be more than a few lattice spacings. Hence, except perhaps for Regime III as discussed below, the conditions for 1d nucleation are almost always met in LH theories.

#### (5) THE REGIME III ANALYSIS FOR ROUGH SURFACES

It was recognized that the rate equation approach (as described above in deriving equation (10) for Regime II) should not be valid in the limit of  $\lambda \rightarrow a$ <sup>15,41</sup>. A list of conditions for its validity was given in Part 1. (A discussion will also be given below in connection with simulation results.) One condition is the need for flat surfaces to exist for the patch initiation process to occur (this gives equation (8)). The following model has been proposed to overcome this particular restriction.

Four adjacent surface sites 'a–d' are considered (for which Figure 5 shows the structure in projection down the stems). Stems are allowed to add to site 'a', then the system progresses either by the removal of that stem or by the addition at site 'b'. In the latter case either the second

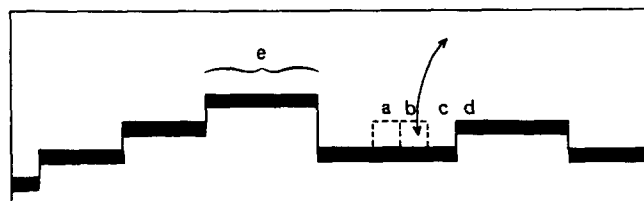


**Figure 5** Schematic representation of a 1d crystal surface in projection down the molecules which is relevant to Regime analyses of LH theories. Sites labelled a–d refer to Regime III; d is a niche site and stems are added in the sequence a–c (the arrow refers to the situation when a stem has arrived at site b, in which case the model allows the stem at b to leave or another stem to arrive at c). Sites e are those which project furthest in the direction of growth (vertical in the diagram)

stem is removed or a third is added at 'c'. Once a stem is in site 'c' the original niche site has disappeared and none of the three stems are allowed to be removed. No addition processes are allowed other than in this sequence of three, e.g., additions are not considered at that part of the growth surface which projects furthest in the direction of growth (Figure 5 at 'e': by definition this cannot have an existing niche). Sets of flux equations were set up analogous to those equations for calculating rates of patch creation<sup>3</sup>, giving:

$$G(\text{III}) = A_0 / (1 + B'_1/A_1 + B'_1{}^2/A_1^2) \quad (18)$$

Unlike equations (8)  $G(\text{III})$  does not go to zero as  $l$  goes to  $l_m$  (see the dotted line in Figure 4) nor does it predict a maximum in  $G$  as a function of  $l$ . An averaged  $l \gtrsim l_m$  was obtained from this model<sup>15</sup> by using an integration over  $G$  which had a lower limit  $l = l_m$ . From the form of the plots of  $G$  in Figure 4 it is clear that the  $l$  value is nearer  $l_m$  for the Regime III formula than for the Regime II one. Consequently  $\delta f$  is smaller and  $B'_1/A_1$  is nearer unity.

The justification of the three sites at the origin of equation (18) is the idea of fold interactions which is documented in detail elsewhere<sup>43-46</sup>. Presumably the analogue for a system where this effect is absent (e.g., paraffins or other oligomers with extended chains) would be a one site niche model and the growth rate would be simply  $A_1$ . (Once one stem is in place it would not be removed, just as the case of polymers the removal rate for a completed triplet of stems is zero.)

For an approximate estimate of  $G$  the denominator in equation (18) is put to unity and:

$$G(\text{III}) \simeq A_0 \quad (19)$$

Computer simulation studies were used to extend the Regime III analysis<sup>16</sup>, using the basic premise that removal events could be neglected. This makes the approach analogous to that used in diffusion controlled aggregation<sup>42</sup>. In addition, the results included data with negative  $\sigma_n$  (creation of 0 type sites is then faster than 1 or 2 type sites). As might be expected, the system then has a driving force to proliferate surface area. In order to eliminate this undesired prediction, a study was made of different lattice symmetries.

## (6) SOME SIMPLE INTERPRETATIONS OF REGIME BEHAVIOUR

The following, while not following the derivations originally given, is useful in assessing the Regime III analyses. It was devised with the substantive help of P. J. Barham. They follow from the fact that, for calculating a growth rate, only attachments at parts of the growth face which project furthest in the growth direction need be considered.

### (i) Regimes I and II

Regime I is when the lateral crystal width  $L \ll \lambda$ . The growth rate is then given simply by:

$$G(\text{I}) = iL/a \quad (20)$$

Regimes II and III correspond to  $\lambda \ll L$ , so that a structure such as that shown in Figure 5 will result. The only part of the growth face (e) which contributes is that which projects furthest in the growth direction bound by niches facing away from each other, and of width  $\sim \lambda$ .

(However,  $\lambda$  refers to the average separation for all types of niches.) In a way analogous to equation (20):

$$G \sim i\lambda/a \quad (21)$$

For  $\lambda \gg a$ ,  $\lambda$  is given by<sup>1</sup>:

$$a/\lambda = 2e^{-\sigma_n/kT} = 2(A_0/A_1)^{1/2}$$

It is readily seen that when this result for  $\lambda$  and  $i$  from equation (8a) are substituted the general form of the  $G(\text{II})$  result is obtained (equations (10) and (11)). (The correspondence is not exact since  $\lambda$  is an average which does not apply to pairs of niches facing away from each other.)

### (ii) Regimes II and III

Regime III could be considered the limiting case where  $\lambda \simeq a$ , so that the width of the furthest protruding part of the face is  $a$ , in which case:

$$G \simeq i \quad (22)$$

The difficulty in implementing equation (22) is how to justify a value for  $i$ , and this difficulty is probably general to many simple analytic approaches to a rough surface. It would certainly not be appropriate to use equations (8) or (8a), which are for patches fluctuating in size on an infinitely wide substrate. If the single site were to continue to increase in height on its own, the result would be a 1d crystal and highly unrealistic. What is more the simulation results<sup>1</sup> show that unless  $\delta f/kT \gg 1$  the lateral correlations between stems on the 1d surface of the 2d crystal are never likely to be negligible, since a roughness approximating to equilibrium is retained. The Regime III result<sup>15</sup> is recovered if  $i$  is replaced by  $A_0$ . Whether this is justified is discussed below. One would then have the three slopes of  $G$  on a log scale against  $\sigma_n/kT$ . (In this model  $\sigma_n/kT$  is approximately equivalent to  $(T\Delta T)^{-1}$ ). Regimes I and III give slopes of unity and Regime II a slope of 1/2.

## (7) AN ALTERNATIVE ROUGH SURFACE RESULT

For the particular case of  $\sigma_n/kT \lesssim 1$  it would be reasonable, as an alternative to equation (22), to assume a limit of very high roughness, in which case all the addition sites are nearly equivalent ( $A_0 \simeq A_1$ , and  $B_0 = B'_1$ ), and:

$$G \simeq \langle A \rangle (1 - e^{-\delta f/kT}) \quad (23)$$

For the transition Regime II to rough surface growth the following alternative approach is suggested by the foregoing. ('Regime III' is reserved for the particular rough surface analysis already published<sup>15</sup>). Regime II is the case where growth occurs at niches which have a steady state density  $C_1$  (rather less than the equilibrium density, see below). The factor  $A_0$  in the Regime II result expresses the fact that  $C_1$  (and hence growth rate) depends exponentially on  $-\sigma_n/kT$ . As  $\lambda$  approaches  $a$ ,  $C_1$  saturates at a value of the order of unity, and no further significant increase in growth rate is possible by increasing  $C_1$ . Equation (23) represents the growth rate in this situation of maximum  $C_1$ .

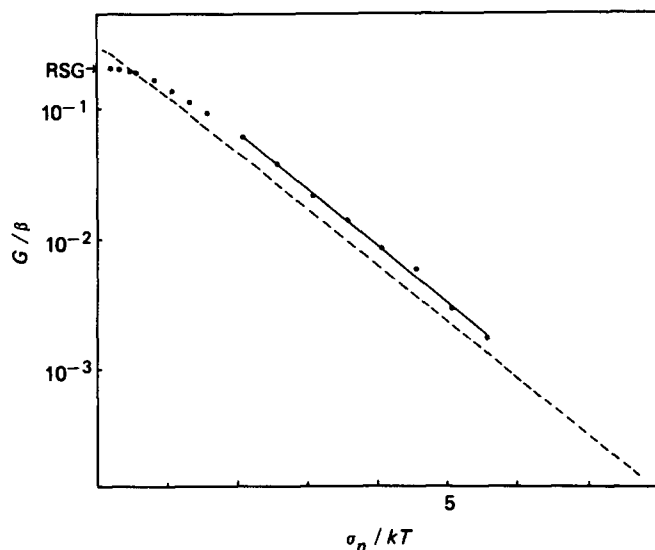


**Figure 6** Normalized growth rates  $G/\beta$  obtained by computer simulation (points and solid line) and by the LH Regime II result (equations (8), (9) and (10)), broken line. The abscissa  $\sigma_n/kT$ , the step free energy, is equivalent in LH theories to  $(T\Delta T)^{-1}$  in the case where  $l \propto \Delta T^{-1}$ ,  $\delta f/kT = 0.24$ . RSG corresponds to a rough surface result (equation (23))

#### (8) COMPARISON OF RESULTS FOR LH REGIME II, SIMULATION, AND NEAR EQUILIBRIUM ( $\lambda \gg a$ )

In this section the emphasis is on how the growth rate  $G$  depends on  $\sigma_n$ . In a complete LH theory  $l$  (and hence  $\sigma_n$ ) are themselves variables determined by the conditions; this question has been treated separately in section (3). For the present purposes it suffices to know that  $l \sim \Delta T^{-1}$ , that  $\sigma_n$  in these models is presumed to be proportional to  $l$ , and hence to  $\Delta T^{-1}$  (equations (5) or (6)) and that  $\delta f/kT$  is somewhat less than unity. The usual format for presenting growth rates is on a log scale against  $(T\Delta T)^{-1}$ ; the equivalent here is to choose  $\sigma_n/kT$  as the abscissa (as was just indicated, the model gives  $\sigma_n/kT \sim \Delta T^{-1}$ ).

The Regime II result is that  $G$  is proportional to  $A_0$  and hence to  $e^{-\sigma_n/kT}$ . The broken line in Figure 6 indicates this result for a constant value of  $\delta f/kT = 0.24$  (and hence constant  $B'_1/A_1$ ). Equation (8) was used, and  $A_0 = A_1$  in order to make direct comparisons possible with the simulation results.

The points indicate results from simulation. For  $\sigma_n/kT \gtrsim 2$  these points also give a linear plot. The slope, from a least squares fit for  $\sigma_n/kT$  values higher than 2, was  $1.01 \pm 0.01$ , and the ratio of the intercept to that for the Regime II plot was  $1.42 \pm 0.03$  i.e.,  $2^{1/2}$ . For small  $\sigma_n/kT$  the reduced growth rate  $G/\beta$  saturates and the intercept at  $\sigma_n = 0$  has a value of 0.21, which is equal to the prediction from equation (23). (RSG denotes rough surface growth.)

The derivation of equation (10) presupposes  $\lambda \gg a$ . The approximate limit of when the plot of the simulation results are parallel to the Regime II result gives  $\lambda \gtrsim 4a$ . This suggests that the condition  $\lambda \gg a$  is not very stringent.

The intercept of the straight line portion of the plot of the simulation results agrees accurately with the prediction of growth in the limiting case approaching equilibrium (equation (13)); this is  $2^{1/2}$  larger than for the Regime II result. This is implicit in the results in Part 1; it was found that (a)  $C_1$  was close to equilibrium values and

that (b) for  $\lambda \gg a$  the growth rate was indeed given by the product  $C_1 g$ . (a) and (b) are the two assumptions made in deriving the 'near equilibrium' result.

The question now arises of why  $C_1$  is near equilibrium (at least for these simulation results), rather than being less than equilibrium, by a factor of  $2^{1/2}$  as calculated by the Regime II analysis. In the latter case it is presumed that only patches, and not cavities, contribute to the creation of niches<sup>11</sup>. One might have expected this at least in the case of 1d nucleation ( $\lambda \gg d$ ), in which case cavities (which are limited in size to about  $d$ ) would not in general grow to a size comparable with the niche separation  $\lambda$ .

Further information is available by considering results for  $B_2 = 0$  (as in Part 1, where this procedure gave different results when conditions for 1d nucleation are not met). For the case of 1d nucleation ( $\lambda \gg d$ ) the growth rates and  $C_1$  values were the same as when  $B_2 \neq 0$ . However, when  $d \gtrsim \lambda$  the growth rates are anomalously large, because of fluctuation effects, and  $C_1$  values are less than the equilibrium value (by a factor of about  $2^{1/2}$ ). Hence in the limit of  $\delta f \rightarrow 0$  ( $d$  large) the Regime II result of a reduced  $C_1$  can be obtained. Paradoxically, however, this agreement with the Regime II  $C_1$  result only happens under conditions where the derivation of Regime II results is not valid because of their neglect of fluctuations!

The conclusion suggests itself of a type of 'kinetic roughening'—one which increases  $C_1$  from below to equal the equilibrium value as the growth rate increases. A more appropriate description would be a growth-mediated approach to equilibrium. During 1d nucleation (i.e., large enough growth rate) enough niches are being generated from patches that the equilibrium  $C_1$  value is attained without the need for cavity creation.

In summary, the LH Regime II using REA result predicts an exponential dependence of  $G$  on  $\sigma_n$  for the 2d model which is reproduced accurately for  $\lambda \gtrsim 4a$  by the simulation results. The values of  $G$  are however lower for LH theories than for the simulation by a factor of  $2^{1/2}$ . This can be attributed, for the case  $\lambda \lesssim d$ , to the omission in LH theories of removal from type 2 sites and of fluctuation effects<sup>1</sup>. For  $\lambda \gg d$  the discrepancy is due to an approach to equilibrium which is mediated by the growth process, whereby  $C_1$  is about equal to the equilibrium value rather than being smaller.

Kinetic roughening, in the sense of  $C_1$  being higher than for equilibrium, is not large for  $\delta f/kT \lesssim 1$ , so that the same would be true for LH theories for polymer crystallization since  $\delta f/kT$  values are then generally smaller than unity. This conclusion would not necessarily apply to the situation where  $l$  values are imposed by the finite molecular chain length, as in PEO<sup>38,39,25</sup>. In this case, the argument given in section 3 giving  $\delta f/kT_m \lesssim 1$ , does not apply.

#### (9) THE SIMULATION RESULTS FOR $\lambda \simeq a$

These confirm the expectation from equation (23): as  $\sigma_n$  is reduced and  $\lambda \rightarrow a$  there is little scope for the growth rate to be further increased by increasing  $C_1$ , and  $G$  levels off (Figure 6). The intercept at  $\sigma_n = 0$  agrees well with equation (23).



## (10) A CRITIQUE OF THE REGIME III ANALYSIS

### (i) Derivation from the model

(a) Only one type of surface site is considered (a–d in Figure 5) whereas a rough surface will have a large range of possibilities. Part 1 has shown that even the neglect of one of the least likely removal events, by setting  $B_2 = 0$ , can have significant effects (for Regime II-like behaviour in that case).

(b) The removal rate constant, once a triplet of stems, a–c in Figure 5, is completed, is zero. A ratio of removal to addition rate constants which is zero can only be properly justified by a free energy difference between the two states concerned being infinite. The model appears to violate the principle of microscopic reversibility since the free energy difference is finite.

The effect of 1 and 2 is clearest for the analogue of a Regime III model for stems with no folds (see section (5)). In that case the growth rate is always  $A_1$ . This can be seen very clearly to lead to the growth rate anomaly as discussed below.

(c) Removal events, even though they may not be numerous enough to affect calculations of  $G$  to the precision usually required, are very important for the determination of surface structure (e.g., niche density). The simulation results show that even for  $\delta f/kT \gtrsim 1$ , where  $B'_1$  is less than  $A_1/e$ , the  $C_1$  values are fairly near the equilibrium values (i.e., those which are found in the limit  $\delta f \rightarrow 0$ ). The modelling of crystallization as an aggregation process (all  $B_i = 0$ )<sup>16</sup> would not be justified unless  $\delta f/kT$  is very large compared with unity. This is not possible for LH theories for polymers, as is shown in section (3).

(d) The Regime III result can be obtained by substituting  $A_0$  for  $i$  in equation (22), but there is no justification for doing this (see also 'interpretation'). This is emphasized by considering the version of Regime III that would be appropriate for the case of no folding. The growth rate is then  $A_1$  (see above), which would give an entirely different dependence of  $G$  on  $\sigma_n$  (and therefore on  $\Delta T$ ).

### (ii) Predictions

(a) The results do not show a maximum in  $G$  versus  $l$ , i.e., a finite  $l$  value is not predicted. A suitable value for  $\langle l \rangle$  is obtained only by the expedient of imposing the range of integration with respect to  $l$ . Positive growth rates are predicted for  $l \leq l_m$ .

(b) The result for  $G$ , in the limit of  $\sigma_n = 0$ , is lower than for Regime II (see also the rough surface result, equation (23)). This is in contrast to applications of the theory where the Regime III result is higher than the Regime II result. This point can be illustrated by neglecting  $B'_1/A_1$  compared with unity for both Regimes II and III, such that  $G(\text{II}) \approx 2^{1/2}\beta$  and  $G(\text{III}) \approx \beta$ . This difference becomes larger still if the additional factor of  $2^{1/2}$  is included than for Regime II (see section (7)):  $G \approx 2\beta$ .

It is true that  $G(\text{III}) > G(\text{II})$  if the formulae are extrapolated to the case of negative  $\sigma_n$ . There would appear to be a basic problem in proposing negative  $\sigma_n$  (see section (5) in connection with ref. 16), since the implication would be a driving force in favour of the creation of additional lateral surface area. This implies that the system is above its critical point, which does not

seem likely for crystals. Even apart from this objection, the prediction of increasingly large growth rates seems to be based on a misleading interpretation of the role of  $A_0$  in the equations (see the section that follows on 'interpretation').

### (iii) Interpretation

The factor  $A_0$  occurs in formulae for growth in Regimes I and II because of the exponential dependence of niche density on  $\sigma_n$ . In the limit  $\lambda \gg a$ , growth rates are calculated as the product of the niche density and niche speed (equation (12)). This interpretation shows that growth will not increase indefinitely as  $\sigma_n$  is decreased: as  $\lambda \rightarrow a$  the niche density will saturate. The Regime III result, by contrast, can be obtained by considering  $A_0$  as simply a kind of attachment frequency which can increase indefinitely as  $\sigma_n$  is decreased. If, as is postulated here, the model should predict  $G$  which saturates in the limit of small  $\sigma_n$  rather than increasing indefinitely, there is no longer a barrier term in the sense discussed in section (3). A model with  $\lambda \approx a$  should not be chain folded with a small value of  $l - l_m$ , since there is then little penalty in growth rate for increasing  $l$ .

## (11) COMPARISON OF LH THEORIES WITH EXPERIMENT

### (i) The $l$ and $G$ values in relation to the form of $\sigma_n$

These theories were devised to explain thickness (and, later, growth rates) and it is interesting to discuss what the essential assumptions are for obtaining results in line with experiment.

In order to predict  $l$  not very much greater than  $l_m$ , LH theories require  $\sigma_n$  to be proportional to  $l$  and to increase to values of more than  $30kT_m^\circ$  (section (3)). The steep exponential decrease of  $A_0$  with  $l$  is necessary to produce a sharp maximum in  $i$  (and hence  $G$ ) at an  $l$  value only slightly greater than  $l_m$ . (If, for example,  $A_0$  were independent of  $l$ , the average  $l$  value produced would be infinite). This form of  $\sigma_n$  is also necessary to explain the temperature dependence of the growth rate. The latter is dominated by  $A_0$ , and the supercooling dependence comes mainly via its dependence on  $l$ . If for simplicity  $l$  is put equal to  $l_m$  (which is proportional to  $\Delta T^{-1}$ ), the growth rate in Regime II (equation (11)) is given approximately by:

$$\begin{aligned} G(\text{II}) &\sim A_0^{1/2} \\ &\sim e^{-\sigma_n/kT} \\ &\sim e^{-\sigma a l_m/kT} \\ &\sim e^{-K_g/T\Delta T} \end{aligned} \quad (24)$$

where  $K_g$  is a constant.

In many cases this approach can give good agreement with many of the trends of  $G$  and  $l$  versus  $T$  (but see also sections (11) subsection (iii)–(v) and (14)). For Regime I  $K_g$  is twice as large, since  $G(I) \propto A_0$ .

### (ii) $\sigma_n$ values estimated from morphology

The results of analyses of 2d crystals illustrated in Figures 1b and 2b have been used<sup>1</sup> to interpret crystal morphology in terms of growth rate as a function of orientation of the growth face (polyethylene, PE, and poly(ethylene oxide), PEO, were chosen as examples).



Use of 2d models in this context does not necessarily imply that the optimum model should be 2d (e.g., *Figures 1a* or *2a*). Clearly, faces which are oblique to the principal crystallographic faces have a higher density of re-entrant corners (steps or niches), and therefore have some consequent enhancement of the growth rate. The simulation results quantify this effect. One example is crystals with curved outlines, in which case it was found that curvature is not consistent with  $\sigma_n$  being very much greater than  $kT$ . For  $\sigma_n$  larger than this, the minima in growth rate around the principal directions are so deep that only faces near the principal ones in orientation would be seen. (Crystals with curved outlines are of course distinct from crystals whose *fold planes* are curved). A second example is some twinned crystals, in which straight faces are generated which do not follow the principal crystallographic faces. One can then read off directly the growth rates for at least one of the planes which does not correspond to a close-packed plane compared with one which does and make comparison with the predictions. The results again are that  $\sigma_n \approx 1-3kT$ . In addition to estimates of magnitudes of  $\sigma_n$ , this approach suggests that  $\sigma_n$  tends to be smaller when  $l$  is larger.

A simple if approximate way to estimate growth rates on faces of different obliquities is from  $i/g$  ratios on the basis of the usual LH approach. For non-close-packed directions  $C_1$  will be a significant fraction of unity (for (11) faces on a square lattice  $C_1=0.5$  has been found by simulation<sup>1</sup>), so that  $G \sim g$ . Hence if the close-packed faces grow in Regime I ( $G=i$ ) the ratio of the growth rates is approximately the ratio of net addition to flat and corner sites ( $i/g$ ). For Regime II the corresponding ratio is  $(i/g)^{1/2}$ .  $i/g$  in LH theories is given very simply in terms of  $A_0/A_1$  (equations (8a) and (9)). This ratio is in turn determined by  $\sigma_n$  (equations (1) and (2) with  $B_0=B_1$ ).

Thus the form of  $\sigma_n$  necessary to explain  $l$  and  $G$  values on the basis of LH theories are quite the opposite to the results derived from the morphology both as regards absolute values and dependence on  $l$ , at least if sets of data taken with different solvents for solution crystallization of polyethylene are compared. For example, curvature in the outlines of crystals of PE starts to become general as  $T$  is increased and  $l$  is in the region of  $200 \text{ \AA}$ <sup>47</sup>. However, equation (5) would predict that  $\sigma_n/kT$  increases to about 20 as  $l$  is increased to these values. Were this to be true, the growth rate on non-close-packed directions would be  $\sim 10^9$  faster than on {110}, compared with observed ratios around unity. Again, the maximum  $\sigma_n$  values found from observation of morphology<sup>1</sup> are in the limit of low  $l$  and  $T$  (and low molecular weight). From equations (5) or (6) for LH theories it is then that  $\sigma_n$  should be *smallest*.

It should be stressed that the conclusions of the analysis of twins are essentially the same as those which have already been reached for PEO<sup>39</sup> using the conventional concepts and notation of LH theories. In this case a twin boundary enhances growth so that two sides of the crystal are straight and the other two slightly roof-shaped, with an apex at twin boundaries which are in the centre of the face. It is readily seen from the shape of the crystal that the oblique faces (the 'roof' section) grows only slightly faster than the others. The original analysis<sup>39</sup> was in terms of a  $g$  value which was much too small relative to  $G$  for LH theories to apply. This, qualitatively, is in agreement with

the present analysis, i.e., that growth on to re-entrant corner sites is only slightly greater than on to other types of site. Once this is established, however, account must be taken of  $\sigma_n/kT$  not being sufficiently large for a rate equation approach in terms of attachment rate ( $i$ ) and niche spreading rate ( $g$ ) to be appropriate (see section (2) and Part 1). Hence simulation methods, or some other approach appropriate to  $\sigma_n/kT$  of the order of unity, must then be used for quantitative results to be obtained.

Examples of morphology have been chosen from polyethylene and poly(ethylene oxide). The conclusions are probably general however, e.g., for solution grown crystals from a very wide range of polymers. 'Good' crystals with ideally straight perimeters are comparatively rare: much more common are morphologies with a variety of re-entrant corners which do not appear to have drastic enhancements of growth as expected from LH theories.

There is ample evidence that LH theories do not account for the range of morphologies observed, but that does not mean that there are not regimes of growth basically equivalent to 1d nucleation. In the limit of low molecular weight of polyethylene ( $M_w=2300$ ) for crystallization from xylene, at high supercoolings, ratios of growth on non-close-packed to close-packed of up to 20-30 have been observed<sup>27</sup>. This suggests  $i/g$  ratios in the region of  $\sim 10^{-3}$  (for Regime II on the close-packed faces). Recently even smaller  $i/g$  ratios  $\approx 10^{-4}$  have been derived for molecular weights of 10 000 of polyethylene crystallized from tetrachloroethylene<sup>48</sup>, using methods of analysis based on twin morphology<sup>23,27</sup>. This solvent has a lower dissolution temperature than xylene with correspondingly lower crystallization temperatures. What is more,  $i$  values decrease markedly as  $\Delta T$  decreases, in line with expectations from LH theories. In this limit of the lowest available crystallization temperature, the regime of crystallization may indeed resemble nucleation as originally conceived. It corresponds to the lowest absolute  $G$  values for a given  $\Delta T$  (see section (14)). However, even in these cases,  $\sigma_n/kT_m^\circ$  as calculated from  $i/g$  (via  $A_0/A_1$ ) is no more than about 4. Furthermore, if equations (5) or (6) were generally applicable, and if current values of  $\sigma$  were to be used,  $i/g$  ratios would decrease drastically as  $l$  was increased above  $\sim 100 \text{ \AA}$ : e.g., for  $l \approx 300 \text{ \AA}$   $i/g$  would be  $\sim 10^{-26}$ , with drastic consequences for rates of growth and morphology.

It is implicit in this section that relative rates of growth for different orientations of growth faces depends only on  $\sigma_n/kT$  (and corresponding  $i/g$  values). Recently it has been proposed<sup>49,50</sup> that curvature can result from 'poisoning' of corner sites (e.g., by very strong attachments of impurities). When an impurity is present the step spreading rate is put to very small values (e.g., zero). A simple interpretation of this approach is to envisage a reduction in the step spreading rates, as averaged over steps with and without impurities, and a consequent increase in effective  $i/g$  ratios (e.g., approaching unity). This impurity effect reduces the growth rate (see section 14)).

The conclusion that nucleation theories were not consistent with the observed lack of influence of niches on growth has been reached by Wunderlich<sup>51</sup> on the basis that niche sites on extended chain crystals were not preferred sites for additional crystallization.

(iii)  $\sigma_n$  and crystal size effect on the growth rate

If there is on average less than one spreading patch on each crystal growth face, it has long been recognized that the growth rate should increase with the lateral crystal size  $L$  (equation (20)). In terms of section (6), the Regime II result assumes a substrate length  $\simeq \lambda$ , and if  $L < \lambda$  then the growth rate will be correspondingly reduced compared with the Regime II result (equations (10–13)). A persistence length  $L_p$  has been introduced on the basis of a hypothetical length on the crystal substrate, the existence of which presupposes a mosaic block crystal structure or defects on the growth face<sup>18</sup>. As long as  $L \gg L_p$  no crystal size effect should be seen on the growth rate.

Point *et al.*<sup>35</sup> have compared predictions of the LH theories with growth rates of polyethylene crystallizing from solution. Even with the existence of a persistence length  $L_p$  they show that their measurements are not consistent with LH theories unless  $\lambda$  ( $=L_k$  in their notation) is no more than an upper bound value of 200 Å. They show that at small times the lateral crystal size  $L$  is proportional to time, and this would not be the case for  $\lambda \gtrsim 200$  Å. (For the other limiting case of  $L_p = L$  and  $\lambda \gg L$ ,  $L$  should increase exponentially with time.)

For Regime II the density of niches is  $2^{-1/2}$  the equilibrium density, i.e.

$$C_1 \equiv a/\lambda(\text{II}) = 2^{1/2} e^{-\sigma_n/kT} \quad (25)$$

The upper limit on  $\lambda$ <sup>35</sup> leads to an upper limit on  $\sigma_n \simeq 3.5kT$ . It is true that for one particular  $l$  value, LH theories could give  $\sigma_n$  values as low as this as long as equation (6) is used rather than equation (5). However, because of the basic assumption of a linear increase in  $\sigma_n$  with  $l$ , with a large constant of proportionality (equations (5) or (6)), the same could not be true for a range of  $l$  values. For example, for PE, using currently accepted values for the input quantities<sup>12</sup>,  $\sigma_n = 3.5kT$  would be consistent with  $l = 91$  Å. This would mean however that if  $l$  were increased even by as little as 30 Å,  $\sigma_n$  would rise to  $6.9kT$  ( $\lambda \simeq 3200$  Å). Since the rise in  $\lambda$  is exponential with  $\sigma_n$  (equation (25)), it is easy to see that equation (6) predicts extremely large  $\lambda$  as  $l$  increases, from values typical of solution crystallization from xylene (105–180 Å) to those for crystallization from the melt (e.g., up to 300 Å or more). Furthermore, if equation (5) is used rather than equation (6) (as Point *et al.* argue is necessary for the self-consistency of LH theories) then all the  $\lambda$  values would be higher by several orders of magnitude, and the discrepancy with observation would be even larger.

The limits put on  $\lambda$ <sup>35</sup> mean that  $\lambda$  is much too small for the growth of these crystals to be in Regime I except when the crystal is extremely small ( $L \lesssim 200$  Å). The preceding paragraph suggests that if equation (6) is used  $\lambda$  is too small for Regime II to apply except for a few particular conditions with appropriate  $l$  values. If equation (5) is used  $\lambda$  is always much larger than the limit found experimentally. The  $K_g$  values derived are also inconsistent with Regime II, since Point *et al.* point out that they require  $\sigma$  values which are higher than those which are usually accepted. Hence neither Regimes I or II of the LH theories seem to be applicable to their data.

## (iv) Growth rate data and Regime changes

Originally the reason for invoking secondary nucleation<sup>52,53</sup> was the straightness of plots of  $G$  on a log

scale versus  $(T\Delta T)^{-1}$  (see equation (24)). More recently, support for nucleation theories has been given in terms of the lack of straightness of such plots. The experimental situation will be summarized for the cases where  $l \propto \Delta T^{-1}$ . A few selected references to growth rate data will be given: more comprehensive bibliographies are given elsewhere<sup>54,55</sup>.

Plots can be straight or approximately so<sup>35,52–56</sup> or can show curvature (convex<sup>57</sup>) or can be made up of two (or perhaps more) straight line portions so as to produce concave<sup>59–62</sup> or convex plots. The ratio of the slopes of the straight lines may be two<sup>62,63</sup> or it may be less than two (1.65)<sup>64</sup>. In other words there is a considerable variety in the form of these plots. In some cases it is possible that some of the detailed features of the plots may depend critically on estimates of  $T_m^\circ$  and on corrections for viscosity terms, which are not straightforward to make.

LH theories can explain convex curved plots on the basis of a Regime I/II transition. In the region of the transition this explanation presupposes that  $\lambda$  is comparable with  $L$  (see section (6) (i)). In at least two cases<sup>65,66</sup> growth rate data consistent with a Regime I/II transition have been observed even when the crystals have curved outlines. In these cases there must be numerous re-entrant corners on the growth face, and in Part 1<sup>1</sup> the analysis of crystal shapes would suggest molecularly rough surfaces ( $\lambda \simeq a$ ). Whatever the precise interpretation of  $L_p$ <sup>18</sup> an explanation in terms of a Regime I/II change would presuppose that  $L_p \gg a$ , in contradiction with the morphological observations.

Figure 7 shows predications in the intermediate region of  $\Delta T$  made on the basis of the analysis by Frank<sup>11</sup>. Such a theory does not explain a sharply kinked growth plot<sup>63</sup>. The prediction of where the transition should take place depends crucially on which equation is used for  $\sigma_n$ . Equation (6) has been used<sup>10</sup> but equation (5) would give an entirely different result (see section (11), subsection (iii)).

Concave plots have been explained on the basis of a Regime II/III transition. However, it is suggested in section (10) that the Regime III derivation is inappropriate and section (7) gives an alternative analysis of rough surface growth using the premises of LH theories. A dependence of  $G$  on  $\Delta T$  is found which is less steep than for Regime II, whereas the Regime III analysis predicted a larger one.

The most direct way of interpreting non-linear growth plots is in terms of a barrier term (whatever its origin) which is proportional to  $e^{-K/l}$  where  $K$  is not necessarily the same for all  $\Delta T$  values (see equation (24)). In terms of LH theories, any growth rate data could be accommodated by adjusting the dependence of  $\sigma_n$  on  $l$ . An increase in  $\sigma_n$  which was faster than the first power in  $l$  would give a convex growth plot, and an increase which was lower would give a concave plot. Section (11) subsection (v) discusses also dependences of  $\sigma_n$  on  $l$  which differ from equations (5) or (6). However, without some physical justification for such adjustments in how  $\sigma_n$  depends on  $l$ , there would be little significance in agreement with experiments which was achieved in this way.

(v) Restricted values of  $l$ : growth rates

Section (11) subsections (i)–(iv) involve  $l$  which

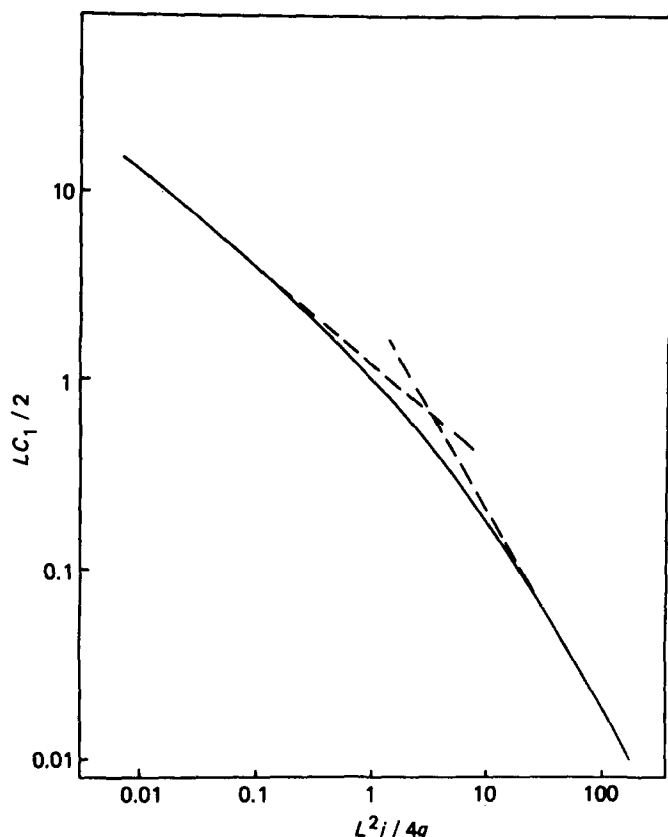


**Figure 7** A plot of dimensionless quantities related to the Regime I/II transition in LH theories calculated from ref. 11.  $LC_1/2$  is proportional to the growth rate since for LH theories  $G = C_1 g$  (equation (12)).  $g$  can be taken to be constant. The log of the abscissa is then related to  $(T\Delta T)^{-1}$  for LH theories. Hence this plot can be compared with a 'growth plot' of  $G$  on a log scale against  $(T\Delta T)^{-1}$ . The ratio of maximum to minimum growth rate ( $10^3$ ) is chosen to be typical of the range of growth rates available experimentally. It can be seen that the predicted curve shows no sharp kink (cf. some experimental data)

changes continuously with  $\Delta T$ . Experimental data are more demanding in terms of a theoretical treatment if restraints are placed on  $l$ , as in the case of oligomers with reasonably small distributions of chain lengths. To some degree the two quantities  $l$  and  $\Delta T$  can then be adjusted independently. In PEO it has been found that  $l$  can be restricted to integer submultiples of the chain length<sup>67</sup>, and very extensive growth rate data are available<sup>39</sup>. Similar if not exactly equivalent effects have recently been observed for PE<sup>59,68,69</sup>. It is found that for the range of  $\Delta T$  where  $l$  is the same, the dependence of  $G$  on  $\Delta T$  is linear rather than exponential<sup>25</sup>. (In some cases of slow growth,  $l$  is likely to increase slightly because of molecular weight fractionation<sup>39</sup>, in which case  $G$  is no longer accurately linear in  $\Delta T$ .) This in principle can be understood on the basis of LH theories (see also section (13) if the parameter  $\psi$  is set to zero. In that case  $A_0$  depends on  $l$  but not directly on  $\Delta T$ . An equation such as equation (11) then gives a dependence of  $G$  on  $\Delta T$  via the term  $(A_1 - B_1)$  which is essentially linear in  $\Delta T$ , at least near the melting point  $T_m$  of the crystals in question (at  $T = T_m$ ,  $A_1 = B_1$ ). This is the approach adopted by Hoffman<sup>20</sup> for PE data, since the  $A_0$  which is used also depends on  $l$  but not directly on  $\Delta T$ . Point and Kovacs<sup>38</sup> consider primarily the question of relative growth rates for different chain lengths (e.g., their Table II for extended chain crystals). The only way of obtaining the steep variation of  $G$  with  $l$  is via the different  $A_0$  values. By

comparing data from pairs of chain lengths, values for  $\sigma$  can be obtained. Equation (26) of that paper derives in essence from a ratio of  $A_0$  values, and is particularly simple for the case  $\psi = 0$ . A range of  $\psi$  values (including 0) is adopted, and a parameter which is 1 or  $1/2$  depending on whether Regime I or II is appropriate is included in the data which are presented. Point and Kovacs state that the apparent  $\sigma$  values obtained from experiments are much smaller than those usually reported.  $\sigma$  values also increase by a factor of about 3 when the average molecular weight of the pair of chain lengths considered is reduced by 2, which is not compatible with equations (5) and (6) (see also section (11), subsection (iv)). They examine alternative assumptions in the data analysis and conclude that the discrepancy between LH theory and experiment is irreducible.

This argument of Point and Kovacs is illustrated by Figure 6 of ref. 25, which is in effect a plot of  $A_0$  versus  $l$  as derived from a large selection of the Kovacs data. If the growth corresponded to LH theories with the same regime (e.g., Regime II), all the points should lie on one master curve with a slope related to  $\sigma$ . It is easily seen that as the number of folds is decreased the growth is much faster than expected on this basis (this is particularly true of extended chain crystals).

The case of oligomers of PEO provide some of the clearest morphological evidence (e.g., the outlines are almost always curved to some degree) and this is discussed in sections (11) (ii) and (13) and elsewhere<sup>25</sup>.

## (12) MODELS FOR CRYSTAL GROWTH BASED ON GROWTH FACES WHICH CAN BE ROUGH AND PINNING

These models are not the primary concern of these papers, but it is informative to discuss their similarities and differences with LH theories.

The models<sup>24,28-30</sup> predict a finite  $l$  value and the temperature dependence of  $G$  along lines which mathematically are very similar to the nucleation model (section (3)). There is a 'barrier term'  $a_0$  which is a steeply decreasing function of  $l$  and a 'driving force term' (linear in  $l$  at small  $l - l_m$ ). Since  $a_0$  is not related directly to  $\sigma_n$ , the model is fully consistent with the crystal shapes.  $a_0$ , as  $A_0$ , depends approximately exponentially on  $l$ <sup>28,29</sup>, leading to the growth rate dependence on  $T$  as shown in equation (24).

The physical basis of the term  $a_0$  will be described briefly: it is the consequence of the geometry of the crystal near the growth face and of likely restrictions due to chain connectivity. Only if stems of the same crystal are presumed to be all the same length will the lamella have a strictly rectangular cross section across the depth of the lamella (Figure 8a). If, for example, stems are considered to be made up of shorter constituent 'units' as shown in Figures 1a and 2a<sup>3,13,22</sup>, general considerations<sup>70,71</sup> and simulation studies<sup>24</sup> show that the profile will be irregular at the corners, i.e., near the growth surface of the lamella (Figure 8b). The profile averaged over all the irregularities will be 'rounded off', the stems near the growth face being generally shorter than in the interior of the lamella (Figure 8c). The restrictions due to connectivity arise since a unit which is to be added to an existing stem cannot be chosen at random (as it can be for non-polymers) but must be the sequence of chain which is

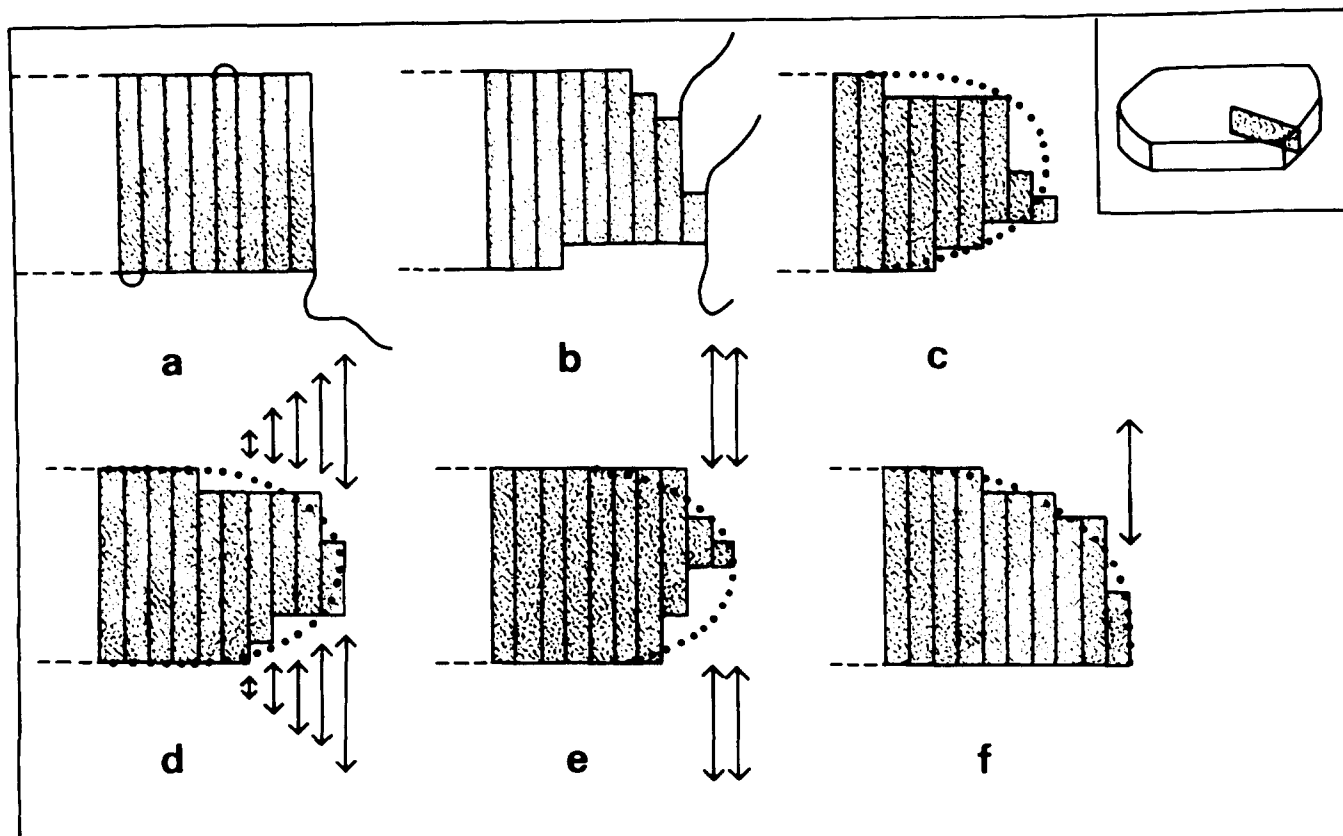


**Figure 8** Schematic description of the cross section of the growth surface of a polymer crystal, as postulated in the roughness pinning models<sup>22-30</sup>. (a) Idealized 'squared-off' structure (this is the structure assumed always to be the case in LH theories). Two folds and a loop are shown, but the details of folding are not of principal interest here

covalently linked to the unit already at the end of the stem. A stem end which coincides with a molecular end<sup>25</sup>, or whose attached chain is pulled taut in a fold or loop<sup>24</sup>, is not capable of extending (it is 'pinned'). Similarly, some stem ends tightly enclosed by others will be pinned for removal events. The essential feature of the model (regardless of the details of pinning) is that restrictions should increase the further the distance behind the growth face. A likely gradation of the restrictions is shown diagrammatically in *Figure 8d* by the arrows of various lengths, though for the purpose of calculations, models such as *Figures 8e* and *8f* have been studied (by Monte Carlo simulation<sup>24</sup>, solution of rate equations<sup>28,30</sup>, and a simple analytic approach<sup>29</sup> respectively).

The high free energy stage leading to the  $a_0$  barrier term is entropic, i.e., the configurations which allow growth are much less numerous than those that do not. The crystal cannot incorporate stems finally until they are about  $l_m$  in length or greater, but the additions can only take place at unpinned stems. For example for the model in *Figure 8* only individual configurations such as in *Figure 8a* ('squared off') allow the growth front to make a net advance. For the other configurations, a net advance would involve large defects being incorporated and a fall in free energy on crystallization would not be obtained. In a sense these other configurations are 'poisoning' the growth, and the more of them there are, the more growth is slowed.

A simple calculation shows<sup>29</sup> that the number of different molecular arrangements which are available to the growth front tends to increase exponentially with  $l$ . Since in the simplest version of these models only one

arrangement allows growth (the squared off arrangement), the growth rate should contain a barrier factor which tends to decrease exponentially with  $l$ .

### (13) SOME COMPARISONS OF THE PINNING/ROUGHNESS MODEL WITH EXPERIMENT

This section provides briefly the equivalent of section (11), though some of the details of the approach are still the subject of continuing study. The trend  $l \sim \Delta T^{-1}$  and the exponential dependence of  $G$  on  $\Delta T$  are calculated, for the three methods of analysis described in section (12). The magnitude of the proportionality constant is in agreement with experiment for PE if the average number of monomers  $n_u$  in one of the basic 'units' considered by the theory<sup>29</sup> is  $\sim 3$ . The  $l$  values are low in magnitude<sup>24</sup> compared with experiment, but this would be expected from the small value of  $l_m$  in the calculations (this follows from the way the energy parameters are included). Equivalent calculations which include high enough energies to correspond to folds in the completed fold surface have yet to be made.

The models were developed with morphology in mind, and with the growth surface roughness one would expect  $\sigma_n/kT \approx 1$ . As  $\sigma_n/kT$  is increased from unity to  $\sim 2.5$ , the morphology which is predicted on the basis of growth rate as a function of orientation of the growth face changes from near to disc shaped to an approximate square with slightly convex sides<sup>1</sup>. Further detailed analysis of the straightness of perimeters involves both 2d models (*Figures 1b* or *2b*) and 3d models (*Figures 1a* and *2a*, and work to be published).

Values of  $\sigma_n/kT$  of 1–2 are suggested<sup>1</sup> by the analysis of twin morphology<sup>27</sup>. The variations of morphology with temperature are not inconsistent with a constant  $\varepsilon$  value (where  $\varepsilon$  is an energy parameter for the bonding of 'units'<sup>22</sup>), with a consequent decrease in  $\varepsilon/kT$  with increasing temperature<sup>1</sup>, but a detailed analysis of this question is likely to involve many specific physical chemical effects of the polymer chain and solvent (see also section (14)). The small values of  $\sigma_n$  are also in agreement with the inferences of small  $\lambda$  from correlations of growth rates and lateral crystal size (section (11) (iii)). By correlating the changes in  $\sigma_n$  as estimated from morphology with theory, Part 1<sup>1</sup> has given  $n_u \approx 5$ , which is in very satisfactory agreement with  $n_u$  estimated quite independently from growth rates (see above).

Although the model predicts a barrier term whose dependence on  $l$  tends to be exponential, there is no reason why the dependence should always involve the same proportionality constant (cf.  $K_g$  in equation (24)). Indeed, by changing an energy parameter  $\varepsilon$  in the calculations<sup>29</sup> one can derive two limiting cases of exponential dependence, with a ratio of roughly two in the constants of proportionality (cf. Regimes I and II). Again, the simulation results<sup>24</sup> can show both linear and convex growth plots, depending on the details of the rules which define the method of pinning mathematically.

The application of the model to PEO (restricted  $l$  values) is treated elsewhere<sup>25</sup>. Both the morphology and the linear dependence of  $G$  on  $\Delta T$  (with fixed  $l$ ) can be explained. There is evidence both for an increase in equilibrium roughness, as indicated by curvature in the growth face as temperature is increased, and for some kinetic roughening over a small range of temperature as  $\Delta T$  is increased. The model does not imply any very specific way in which growth rates should vary for different  $l$  values (cf. section (11) subsection (v)) and in fact the summary of growth rate data in *Figure 6* of ref. 25 will probably be one of the best bases for elucidating the particular ways the pinning may be operating.

#### (14) REDUCED GROWTH RATES: $G$ FOR EQUIVALENT $\Delta T$

It has only been pointed out recently in an explicit manner<sup>23</sup> that PE crystals crystallize from the liquid state about 1000 times faster than from solution<sup>12</sup> for the same  $\Delta T$  values. This observation has now been extended to solutions with dissolution temperatures higher<sup>65</sup> and lower<sup>49</sup> than for xylene, and the same trend is clear: the higher the temperature the higher the 'reduced growth rate'. The factors of increase are almost certainly larger than one would expect purely from transport of segmental motion terms.

There is nothing in LH theories which seems capable of explaining this large dependence of  $G$  on absolute temperature which seems to be superimposed on the  $\Delta T$  dependence. However, the pinning/roughness approach would predict such a trend in a very natural way, since smoother surfaces (lower  $T$ ) will generally tend to give lower growth rates.

The details of the dependence of roughness on  $T$  are not yet clear (roughness on crystal surface is a complex phenomenon even for non-polymers). Increasing roughness is usually associated with a decrease in  $\varepsilon/kT$  where  $\varepsilon$  is an effective energy of bonding for each unit<sup>22</sup>.

Growth from different solvents changes  $T$  and hence  $\varepsilon/kT$ , and it is possible that this alone could account for differences in morphology<sup>1</sup>. However, there are likely to be additional effects on  $\varepsilon$  by changing solvent. A complete thermodynamic treatment of crystallization from solution would require that  $\varepsilon$  take into account a range of effects (solvent interactions, 'unit' size, molecular weight and so on). If  $T$  were to be the only variable of importance, the effects of absolute temperature in speeding growth and modifying  $\sigma_n$  and  $i/g$  ratios should be superimposed on those of  $\Delta T$ , and the growth plots (section (11) subsection (iv)) would be correspondingly modified. Kinetic roughening (as defined in Part 1<sup>1</sup>) may also be significant (e.g. Ref. 25, in connection with morphology). Details such as these are still under study.

#### (15) MINIMA IN CRYSTALLIZATION RATES AS A FUNCTION OF SUPERCOOLING

Minima in the rates both of primary nucleation and growth have recently been found for long chain paraffins<sup>72</sup>, and this is probably unprecedented in crystal growth. A rate equation approach based on a simple version of the roughness/pinning model<sup>28</sup> has been able to predict minima (Sadler and Gilmer, reference 73). The interpretation of these calculations is closely similar to the explanation given by Ungar<sup>72</sup>, that thin crystals (e.g., of once folded chains) which are almost but not quite stable at the crystallization temperature can 'poison' the growth of thicker crystals (e.g., crystals of extended chain crystals). This is clearly related to the entropy barrier as discussed in connection with *Figure 8* (section (12)). The LH theories would appear to be incapable of explaining minima in these growth processes.

#### (16) SIMPLIFICATIONS USED IN THE MODELS

All the models discussed here have some simplifying assumptions in common. They all use a lattice with nearest neighbour bonding. Many effects which may have an influence (particularly on specific polymers) are omitted. For example the alkane lattice is known to undergo many subtle transformations e.g., on heating. In ref. 22 it was pointed out, for this reason, that 'surface effects may induce changes in structure which are not apparent in the bulk'. The issue of how typical the molecular structure in the surface is of the interior structure is a very general one with no absolutely clear answers even for non-polymers. However, models with nearest neighbour bonding have certainly been useful for non-polymers, in spite of (and perhaps because of) their simplicity<sup>31–33</sup>; e.g. the concept of a surface step is important in crystal growth. Equally, some of the principal trends in polymer crystallization may be accessible to models with nearest neighbour bonding. In support of this is the observation that a wide range of polymers share many of these trends in spite of entirely different local structures.

The same issue of simplicity *versus* complexity arises for other aspects of the models, since none of them can take account of the full complexity of polymer crystals. Neither LH nor roughness/pinning models contain molecular connectivity explicitly, and can be applied with little modification to the crystallization of extended chain crystals. In LH theories the connectivity only arises *via* the free energy of the fold surface and a simple adjustment

of its value makes the theories applicable to extended chain crystals of oligomeric materials. Again, pinning is the only way connectivity features in the roughness/pinning models. In the 2d analogues of the 3d structures (Figures 1b and 2b) even the pinning is absent. This lack of detail concerning folding may not in itself be a reason for a model to be inapplicable. In support of this is the fact that observation on extended chain crystals of PEO fit into the general pattern which includes crystallization with folding.

For both questions raised here, of nearest neighbour only bonding, and incomplete allowance for connectivity, we should not prejudge the models according to whether they omit some of the complications. The best criterion for a useful model is whether it accounts in a natural way for the main trends which are observed experimentally.

## (17) DISCUSSION AND CONCLUSIONS

This paper sets out to consider four interrelated questions. (i) Simulation methods are used on the basis of the basic premises of LH theories, in order to test whether the rate equation methods (REA) which have previously been employed are likely to be adequate. (ii) Simulation methods are used so as to derive  $\sigma_n$  values from crystal morphology, in a way which is as independent as possible of theoretical models. The contrast between the results and the basic premises of the LH theories is then discussed. (iii) Some other analyses and critiques of LH theories are reviewed and their conclusion related to the rest of this paper. (iv) A brief account is given of the pinning/roughness models at their current state of development and the way that criteria, which have been used for the LH theories, can be applied to them also.

### (i) The rate equation analysis

This analysis for the growth of 2d crystals in LH theories presupposes a regime of '1d nucleation' where patch creation and spreading can be treated as separate processes. Part 1 and section (4) give quantitative criteria which indicate when this is no longer the case. The simulation results for growth rates show no discontinuity according to whether the conditions hold for 1d nucleation, and lead to the conclusion that a result similar to the Regime II one can be derived in a more general way than hitherto. Such a new derivation is based on an equilibrium step density multiplied by the average step speed. The surprising result from the simulation data and this new derivation is a  $2^{1/2}$  increase in the step density and hence in the growth rate compared with Regime II.

The simulation results indicate an approach to equilibrium which is mediated by the growth process, which is absent in the REA. (In the latter case the lack of one source of steps—from cavity creation—can be seen to lead to a steady state step density lower than in equilibrium). It is possible that this conclusion is specific to one particular choice of the apportioning as defined in Part 1. The apportioning reflects the ambiguity in defining rate constants even with the necessary constraint that the ratio of addition to removal rate constants  $A_i/B_i$  reflects the corresponding Boltzmann factor. Either  $A_1 = A_0$  and  $B_0 > B'_1$  (simulation and the REA results in Figure 6) or  $B_0 = B'_1$  and  $A_0 < A_1$  (the usual LH REA choice which is retained for ease of comparisons

in most of the discussion of LH theories in this paper). (The other question in apportioning is equivalent to the choice of the value of  $\psi$ ,<sup>12</sup> which is effectively set to zero in this paper.)

It is interesting to note that in Regime II there is no kinetic roughening, in the sense used here and in Part 1: the step density is always  $2^{-1/2}$  times the equilibrium density.

The simulation results lead to the conclusion that the Regime III rate equation analysis (for rough 1d surfaces) is inadequate. A detailed discussion is given of why this should be so, and it seems clear that the details of the simulation (e.g., apportioning) is not relevant to the discrepancies between the approaches. The most notable reason for the discrepancies is the lack of microscopic reversibility which can be seen on inspection of the Regime III model: the addition process which completes a triplet of stems is not matched by an allowed removal process. The predictions of the revised rough surface result are the opposite of the Regime III ones in that the dependence of growth rate on  $\Delta T$  is less than in Regime II. A consequence of this is a difficulty for accounting for concave growth plots on the basis of LH theories (section (11) subsection (iv)). It is also pointed out in section (11) subsection (iv) that convex growth plots which show a sharp break between two straight line sections cannot be explained by a Regime I/II LH analysis.

### (ii) The application of simulation results to crystal morphology

This shows the inadequacy of the two fundamental premises of LH theories:  $\sigma_n/kT$  is not in general large, nor does  $\sigma_n$  increase steeply and linearly with  $l$  (cf. equations (5) or (6)). With the benefit of hindsight, these premises seem rather unlikely. It has been assumed that the niches are steps which are completely straight, unlike steps on the surface of any other crystal which most certainly have jogs<sup>31</sup>. Only by eliminating the disorder associated with these jogs can the step entropy be ignored and the step free energy  $\sigma_n$  be approximated as the step energy  $\sigma a l$  (equation (5)). It would in fact be very odd if the steps were to be so much more perfectly ordered for polymer crystals than for any other crystals.

### (iii) Some other critiques of LH theories

Other critiques also focus on these two central premises. The lack of effect of crystal lateral size  $L$  on the growth rate leads rather directly to relatively small upper limits for values of  $\lambda$  and hence for  $\sigma_n/kT$ . These experiments also fail to detect the very dramatic increase in  $\lambda$  with  $l$  which is predicted by LH theories. The analysis of growth rates of PEO also show that the relative rates of crystals of different thickness are not consistent with formulae such as equations (5) and (6) which presume a linear increase of  $\sigma_n$  with  $l$ .

### (iv) Models with allowance for growth surfaces and pinning

These models have been reviewed. The idea of growth surface roughness was introduced to account in a qualitative way for curved crystal outlines<sup>22</sup>. The inclusion of pinning enables simple models<sup>24,25,28,30</sup> to account for the overall dependence of  $G$  on  $\Delta T^{-1}$ . Part 1 has shown how simple models with  $\sigma_n$  values much smaller than in LH theories can be used to predict crystal



shapes similar to those found experimentally. This includes the case of twin morphologies which are particularly straightforward to analyse, and the increase in curvature on increasing temperature. The linear dependence of  $G$  on  $\Delta T$  when  $l$  is held constant is explained in a very natural way and the complex pattern of morphological changes in PEO can be explained. Convex growth plots, as well as linear plots, have been obtained from simulation studies<sup>24</sup>, and an analytical approach<sup>29</sup> has indicated that the slope of  $G$  on a growth plot can be expected to change (cf. Regime analyses). Two striking effects, which have recently come to the fore, appear to provide strong evidence in favour of the new approach: changes in growth rates for comparable  $\Delta T$  (section (14)) and the existence of minima in growth rates as a function of temperature (section (15)). Estimates of  $n_u$  (the number of  $\text{CH}_2$  per 'unit' for polyethylene) are in agreement using two independent methods: growth rates<sup>29</sup> and changes in morphology with temperature<sup>1</sup>.

The central issue is of which of the two types of kinetic theory is most productive for interpreting polymer crystallization. Almost any model can lead to occasional discrepancies with experiment, and modifications to some of the details is often a reasonable response to such discrepancies. The burden of this paper is that for LH theories the discrepancies are now both too numerous and too closely related to their fundamental premises for this to be done.

## ACKNOWLEDGEMENT

The author wishes to thank Dr A. Toda for communication of data prior to publication.

## REFERENCES

- Sadler, D. M., Part 1, *J. Chem. Phys.* (July 1987)
- Lauritzen, J. J. and Hoffman, J. D. *J. Res. Natl. Bur. Stand.* 1960, **A64**, 73
- Frank, F. C. and Tosi, M. *Proc. Roy. Soc., London* 1961, **263A**, 323
- Lauritzen, J. I., DiMarzio, E. A. and Passaglia, E. *J. Chem. Phys.* 1966, **45**, 44
- Lauritzen, J. I. and Passaglia, E. *J. Res. Natl. Bur. Stand.* 1967, **71A**, 261
- Hoffman, J. D., Lauritzen, J. I., Passaglia, E., Ross, G. S., Frohnen, L. J. and Weeks, J. J. *Kolloid Z. Z. Polym.* 1969, **231**, 564
- DiMarzio, E. A. *J. Chem. Phys.* 1967, **47**, 3451.
- Sanchez, I. C. and DiMarzio, E. A. *Macromolecules* 1971, **4**, 677
- Lauritzen, J. I. and Hoffman, J. D. *J. Appl. Phys.* 1973, **44**, 4340
- Lauritzen, J. I. *J. Appl. Phys.* 1973, **44**, 4353
- Frank, F. C. *J. Cryst. Growth* 1974, **22**, 233
- Hoffman, J. D., Davies, G. T. and Lauritzen, J. I. in 'Treatise on Solid State Chemistry', Ed. N. B. Hannay, Plenum, New York, 1976
- Point, J. J. *Macromolecules*, 1979, **12**, 770
- Hoffman, J. D. *Polymer* 1982, **23**, 656
- Hoffman, J. D. *Polymer* 1983, **24**, 3
- Guttman, C. M. and DiMarzio, E. A. *J. Appl. Phys.* 1983, **54**, 5541
- Goldenfeld, N. *J. Phys.* 1984, **17A**, 2807
- Hoffman, J. D. *Polymer* 1985, **26**, 803, 1763
- Toda, A., Kiho, H., Miyaji, H. and Asai, K. *J. Phys. Soc. Jpn.* 1985, **54**, 1411
- Hoffman, J. D. *Polymer* 1986, **27** (Commun.), 39
- Hoffman, J. D. *Macromolecules* 1986, **19**, 1124
- Sadler, D. M. *Polymer* 1983, **24**, 1401
- Sadler, D. M. *Polymer* 1984, **25** (Commun.), 196

- Sadler, D. M. and Gilmer, G. H. *Polymer* 1984, **25**, 1446
- Sadler, D. M. *J. Polym. Sci. Polym. Phys. Edn.* 1985, **23**, 1533
- Sadler, D. M. *Polymer* 1986, **27**(Commun.), 140
- Sadler, D. M., Barber, M., Lark, G. and Hill, M. J. *Polymer* 1986, **27**, 25
- Sadler, D. M. and Gilmer, G. H. *Phys. Rev. Lett.* 1986, **56**, 2708
- Sadler, D. M. *Nature* 1987, **326**, 174
- Sadler, D. M. and Gilmer, G. H. *Phys. Rev. B* in press (1987)
- Leamy, H. J., Gilmer, G. H. and Jackson, K. A. in 'Surface Physics of Materials', Ed. J. M. Blakely, Academic Press, New York, 1975, Vol. I
- Weeks, J. D. and Gilmer, G. H. *Adv. Chem. Phys.* 1979, **40**, 157
- Muller-Krumbhaar, H. *Adv. Solid State Phys.* 1979, **29**, 1
- Avron, J. E., Balfour, L. S., Kuper, C. G., Landau, J., Lipson, S. G. and Schulman, L. S. *Phys. Lett.* 1980, **45**, 814-817
- Point, J. J., Colet, M. Ch. and Dosiere, J. *Polym. Sci. Polym. Phys. Edn.* 1986, **24**, 357
- Jones, D. H., Latham, A. J., Keller, A. and Girolamo, M. J. *Polym. Sci. Polym. Phys. Edn.* 1973, **11**, 1759
- Dreyfuss, P. and Keller, A. J. *Polym. Sci. Polym. Phys. Edn.* 1973, **11**, 193
- Point, J. J. and Kovacs, A. J. *Macromolecules* 1980, **13**, 399
- Buckley, C. P. and Kovacs, A. J. in 'Structure of Crystalline Polymers', (Ed. I. H. Hall), Applied Science, London, 1983
- Volmer, M. Z. and Weber, Z. *Phys. Chem.* 1925, **119**, 277
- Phillips, P. J. *ACS Polym. Prepr.* 1979, **20**, 483
- Whitten, T. A. and Sander, L. M. *Phys. Rev. Lett.* 1981, **47**, 1400; *Phys. Rev. B* 1983, **B27**, 5686
- Frank, F. C. in 'Growth and Perfection in Crystals' (Conf. Proceedings on Crystal Growth). Eds. R. H. Doremus, B. W. Roberts and D. Turnbull, John Wiley, New York, 1958, pp 529 and 53
- (a) Frank, F. C. *Disc. Faraday Soc.* 1979, **68**, 7
- (b) Guttman, C. M., Hoffman, J. D. and DiMarzio, E. A. *ibid* p. 297
- (c) Sadler, D. M. *ibid* p. 106
- Flory, P. J., Yoon, D. Y. and Dill, K. A. *Macromolecules* 1984, **17**, 862
- Guttman, C. M., DiMarzio, E. A. and Hoffman, J. D. *Polymer* 1981, **22**, 1466
- Organ, S. and Keller, A. J. *Mater. Sci.* 1985, **20**, 1571, 1602
- Toda, A. and Kiho, H. *J. Phys. Soc. Jpn.* (submitted)
- Toda, A. *J. Phys. Soc. Jpn.* 1986, **55**, 3419
- Toda, A. *Polymer*, in press
- Wunderlich, B. *Disc. Faraday Soc.* 1979, **68**, 239
- Flory, P. J. and McIntyre, A. D. *J. Polym. Sci.*, 1955, **18**, 592
- Burnett, B. B. and McDevit, W. F. *J. Appl. Phys.* 1957, **28**, 1101
- Lovinger, A. J., Davis, D. D. and Padden, F. J. *Polymer* 1985, **26**, 1595
- Toda, A., Miyaji, H. and Kiho, H. *Polymer* 1986, **27**, 1505
- Magill, J. H. *J. Polym. Sci. Polym. Phys. Edn.* 1969, **7**, 1187
- Keller, A. and Pedemonte, E. *J. Cryst. Growth* 1973, **18**, 111
- Cooper, M. and St. J. Manley, R. *Macromolecules* 1975, **8**, 219
- Leung, W. M., St. J. Manley, R. and Panaras, A. R. *Macromolecules* 1985, **18**, 760
- Dalal, E. N. and Phillips, P. J. *J. Polym. Sci. Polym. Lett. Edn.* 1984, **22**, 7
- Miller, R. L. and Seeley, E. G. *J. Polym. Sci. Polym. Phys. Edn.* 1982, **20**, 2297
- Clark, E. J. and Hoffman, J. D. *Macromolecules* 1984, **17**, 878
- Hoffman, J. D., Frohnen, L. J., Ross, G. S. and Lauritzen, J. I. *J. Res. Natl. Bur. Stand.* 1975, **79A**, 671
- Rensch, G. J., Phillips, P. J., Vatansever, N. and Gonzalez, A. *J. Polym. Sci. Polym. Phys. Edn.* 1986, **24**, 1943
- Organ, S. and Keller, A. J. *Polym. Sci. B, Polym. Phys. Edn.* 1986, **24**, 2319
- Labag, J. J., *Thesis*, Strasbourg, 1978
- Arlie, J. P., Spegt, P. and Skoulios, A. *Macromol. Chem.* 1966, **99**, 160; 1967, **104**, 212
- Ungar, G., Stejny, J., Keller, A., Bidd, I. and Whiting, M. C. *Science* 1985, **229**, 386
- Ungar, G. and Keller, A. *Polymer* 1986, **27**, 1835
- Herring, C. *Phys. Rev.*, 1951, **82**, 87
- Frank, F. C. in 'Metal Surfaces', Eds. W. D. Robertson and N. A. Gjostein, American Society for Metals, Metals Park, Ohio, 1963
- Ungar, G. and Keller, A. submitted to *Polymer*
- Sadler, D. M. and Gilmer, G. H. *Polymer (Commun.)*, in press